Tumour cell-induced senescence-like state of macrophages plays a pivotal role in tumour stable growth after tumour cell emergence in immunocompetent condition

Haruka Wada (wada@igm.hokudai.ac.jp)
Hokkaido University
Ryo Otsuka
Hokkaido University
Wilfred Germeraad
Maastricht University Medical Centre
Tomoki Murata
Hokkaido University
Toru Kondo
Hokkaido University
Ken-ichiro Seino
Hokkaido University

Research Article

Keywords: Tumour-initiating cells, immunocompetent condition, macrophage, senescence, CD38, nicotinamide mononucleotide

Posted Date: November 9th, 2022

DOI: https://doi.org/10.21203/rs.3.rs-2236823/v1

Abstract

Background: The cancer stem cell theory proposes that tumour formation in vivo is driven only by specific tumour-initiating cells having stemness; however, clinical trials conducted to test drugs that target tumour stemness have provided unsatisfactory results thus far. Recent studies showed clear involvement of immunity in tumours; however, the requirements of tumour-initiation followed by stable growth in immunocompetent individuals remain largely unknown.

Methods: To clarify this, we used two similarly induced glioblastoma lines, 8B and 9G. They were both established by overexpression of an oncogenic H-RasL61 in p53-deficient neural stem cells. In immunocompromised animals in an orthotopic transplantation model using 1000 cells, both show tumour-forming potential. On the other hand, although in immunocompetent animals, 8B shows similar tumour-forming potential but that of 9G's are very poor. This suggests that 8B cells are tumour-initiating cells in immunocompetent animals. Therefore, we hypothesised that the differences in the interaction properties of 8B and 9G with immune cells could be used to identify the factors responsible for its tumour forming potential in immunocompetent animals and performed analysis.

Results: Different from 9G, 8B cells induced senescence-like state of macrophages around tumours. We investigated the senescence-inducing factor of macrophages by 8B cells and found that it was IL-6. Such senescence-like macrophages produced Arginase-1, an immunosuppressive molecule known to contribute to T cell hyporesponsiveness. The senescence-like Mφs highly expressed CD38, a nicotinamide adenine dinucleotide (NAD) glycohydrolase associated with NAD shortage in senescent cells. The addition of nicotinamide mononucleotide (NMN), a NAD precursor, in vitro inhibited to induction of macrophage senescence-like phenotype and inhibited Arginase-1 expression resulting in retaining T cell function. Moreover, exogenous in vivo administration of NMN after tumour inoculation inhibited tumour-initiation followed by stable growth in the immunocompetent mouse tumour model.

Conclusions: We identified one of the requirements for tumour-initiating cells in immunocompetent animals. In addition, we have shown that tumour growth can be inhibited by externally administered NMN against macrophage senescence-like state that occurs in the very early stages of tumour-initiating cell development. This therapy targeting the immunosuppressive environment formed by macrophage senescence-like state is expected to be a novel promising cancer therapeutic strategy.

Background

Tumour cells in cancerous tissue are heterogeneous. The theory of tumour-initiating cells (or cancer stem cells) may explain an important aspect of the phenotypic and functional heterogeneity among cancer cells in some tumours [1]. According to this theory, only specific tumour cells can initiate stable tumour formation *in vivo*. These cells are less sensitive or more resistant to anti-cancer drugs [2] and have repopulating potential [3] [4]. Therefore, they are thought to be responsible for relapse in many patients [2]. Thus, targeting these tumour-initiating cells are an important therapeutic strategy against cancer

[5] [6]. Many types of tumour-initiating cells, defined by their surface markers or selective gene expression, have been identified [7] [8]. Several reports suggested that Stat3 contributes to self-renewal of the cells as well as tumorigenicity, indicating that Stat3 expression is correlated with the tumour-initiating capacity in some tumour types [9] [10] [11]. Therefore, targeting Stat3 was assumed to a promising therapeutic strategy. However, no improved overall survival was achieved when targeting Stat3 in phase III clinical trials (ClinicalTrials.gov Identifier: NCT01830621 (or results still have to be reported: NCT02178956, NCT02753127, and NCT02993731)).

Although tumour-initiating cell identification has most often been performed in immunodeficient animals, the current general concept is that immune cells are one of the most important components in tumour tissue and suggests that they affect the outcome of tumour treatment [12] [13]. The assumption can thus also be made that the host immune system would influence tumour-initiation. Quintana et al. [14] have reported that a detectable frequency of tumour cells manifests efficiently depending on the host's increased level of immunocompromise. Therefore, a tumour formation can be initiated only from tumour cells that are resistant to the attack of host immune systems, and such tumour cells are perceived as tumour-initiating cells. According to these notions, the character of tumour-initiating cells is substantially influences by the host immune system. In contrast to immunocompromised mice frequently used as model in tumour-initiation research, normal individuals have a good functioning immune system. This may be the reason for failure of clinical studies targeting tumour-initiating cells. In other words, the tumour-initiating cells identified in immunodeficient mice and their mechanisms are often not applicable to immunocompetent individuals. Therefore, to understand tumour biology and develop a novel therapy, it is very important to identify the features of tumour cells which can initiate and form a tumour in healthy individuals and to clarify the mechanism(s) that support such tumour cells' survival.

Although there are various definitions of classes or types for tumour-initiating cells, in this study, we focused on the phenomenon after emergent de novo tumour cells, we analysed the requirement of "tumour-initiating cells" that start and stably form tumour mass in immunocompetent animals.

Methods

Cells and cell culture

Induced glioblastoma cell lines were cultured in media as previously described [15]. All cell lines were cultured at 37°C with 5% CO_2 in appropriate culture medium. Knockout of the IL-6 gene in 8B cells was performed using the CRISPR/Cas9 system (OriGene Technologies, Inc., Rockville, MD, USA).

Mice

Male C57BL/6 mice, female BALB/c, and male BALB/$c^{nu/nu}$ mice (nude mice) were purchased from Japan SLC, Inc. (Shizuoka, Japan). NOD/ShiJic-*scid* mice (NOD/SCID mice) were purchased from CLEA Japan, Inc. (Tokyo, Japan). All animal procedures were approved by the Hokkaido University Animal Care Committee.

In vivo tumour-initiating capacity analysis

Tumour cells (1000 cells) in 3 mL saline were transplanted into the anaesthetised mouse brain using a Hamilton syringe through a skull hole formed by drilling. The cells were injected into the mouse brain over a period of 30 s; the syringe was left in place for another 30 s. Mouse overall survival was analysed by the Kaplan-Meier method. Multiple testing corrections were carried out using the Bonferroni method. The p values <0.05/6=0.0083 (Bonferroni correction) was considered as statistically significant. NS represents non-significant.

Immunohistochemical analysis

Brain samples were embedded in Tissue-Tek OCT (Sakura Finetek, Torrance, CA, USA). 5-μm-thick sections were used. For combined staining of SA-β-Gal and haematoxylin and eosin, SA-β-Gal staining [16] performed at first, then the sections were stained with haematoxylin and eosin. For combined staining of SPiDR-βGal and F4/80, staining of SPiDR-βGal was performed at the same time as staining of the secondary antibody. For immunohistochemical analysis, the sections were stained with primary antibody and then treated with an appropriate secondary antibody conjugated with Alexa488/Alexa555/Alexa647 (Thermo Fisher Scientific). The antibodies used were as follows: anti-CD3 (17A2), -F4/80 (BM8), and -CD38 (90). These primary antibodies were purchased from BioLegend (San Diego, CA, USA). The FITC-conjugated anti-CD3ζ (H146-968) monoclonal antibody was purchased from Abcam (San Francisco, CA, USA). Nuclei were counterstained with 4’,6-diamidino-2-phenylidole dihydrochloride (DAPI; Sigma Aldrich, St. Louis, MO, USA). For multiple immunofluorescent staining, the Opal 4-color fluorescent IHC kit (Perkin-Elmer) was used.

Conditioned medium culture experiment

Glioblastoma cells (8×10^6 cells) were cultured in 10 mL glioblastoma medium. After 4 days of culture, the supernatant was collected and filtered through a 0.45-mm filter. The culture supernatant containing 20% (v/v) fresh glioma medium was used as conditioned medium. $F4/80^+$ cells were magnetically sorted using the MACS system (Miltenyi Biotec GmbH, Bergisch Gladbach, Germany). For RT-qPCR, M0, M1, or M2 Mφs were prepared from splenic $F4/80^+$ cells as previously described. [17]

Flow cytometry

Flow cytometry was performed using an FC500 instrument (Beckman Coulter, Brea, CA, USA) or BD FACSCelesta™ (BD Biosciences, Franklin Lakes, NJ, USA); data were analysed using FlowJo software (Tree Star, Ashland, OR, USA). Anti-mouse CD3 (17A2), CD4 (RM4-5), CD8 (53-6.7), CD45R (RA3-6B2), CD11b (M1/70), CD11c (N418), F4/80 (BM8), and Ly6g (1A8) were used; corresponding isotype controls were purchased from BioLegend. For analysis, live cells were gated based on forward and side scatter as well as lack of DAPI or propidium iodide uptake. All antibodies were used at 1:100 dilutions.

Cell proliferation assay

Whole splenocytes from C57BL/6 mice were stained with 5-(and -6)-carboxyfluorescein diacetate succinimidyl ester (CFSE) (Dojindo, Kumamoto, Japan) and then co-cultured with 8B or 9G for 4 days. To identify the proliferation of various immune cell lineages, we stained the resulting cells with various immune cells markers; CFSE reduction in each immune cell was flow cytometrically measured.

Senescence-associated b-galactosidase assay (SA-b-Gal assay)

Cells or tissue sections were fixed with 4% paraformaldehyde for 10 min; then, 0.5 mg/mL of X-Gal in 5 mM potassium ferricyanide, 5 mM potassium ferrocyanide, and 2 mM $MgCl_2$ solution was added. The cells were incubated at 37℃ for 16 h. After incubation, the cells were washed with PBS and evaluated under a microscope. In the combination of immunofluorescence staining and SA-β-Gal assay, a SPiDER-βGal kit (Dojindo) was used. SA-β-Gal positive or F4/80 positive areas as well as their merged areas were calculated using Image J software. Ten independent regions were analysed, and the means were compared using the unpaired Student's *t*-test.

RT-qPCR

RNA was isolated using Tripure Isolation Reagent (Roche, Basel, Switzerland). Reverse transcription was carried out using ReverTra Ace qPCR RT Master Mix (Toyobo, Shizuoka, Japan). qPCR analysis was performed using a KAPA SYBR Fast qPCR Kit (KAPA Biosystems, Inc., Wilmington, MA, USA) and Step One Real-Time PCR System (Applied Biosystems, Foster City, CA, USA). Primer sequences information will be provided on request.

Morphological analysis of Mφs

For smear preparations, Cytospin (Thermo Fisher Scientific, Waltham, MA, USA) was used; Diff-Quik (Sysmex Corporation, Kyoto, Japan) was used for staining. Specimens were observed via optical microscopy.

Cytokine array

For cytokine array analysis, 8×10^6 glioblastoma cells were cultured in 10 mL glioblastoma medium. After 4 days of culture, the supernatant was collected and filtered through a 0.45-μm filter. The supernatants were analysed by Legendplex (BioLegend) using an FC500 instrument.

Identification of cytokine(s) secreted by 8B that induce Mφs into a senescence-like state

Splenocytes were cultured in media containing 8B-secreting cytokines. We used glioma medium, which is the same as 8B or 9G culture medium. To ensure Mφs survival, M-CSF (5 ng/mL) and IL-34 (5 ng/mL) were added to the glioma medium (base-medium). To identify the factor(s) responsible for Mφs' senescence, we prepared base-medium containing major factors secreted by 8B, including Ccl2 (20 ng/mL), Cxcl1 (5 ng/mL), Cxcl10 (5 ng/mL), Ccl5 (5 ng/mL), and IL-6 (1 ng/mL) (all factors) All cytokines were purchased from BioLegend. We then analysed the effect of removing individual factors on the

induction of senescent Mφs. The concentration of cytokines/chemokines was determined by cytokine array. The generated Mφs were analysed by the SA-b-Gal assay.

Knockout of IL-6 from 8B cells using the CRISPR/Cas9 system

To knockout IL-6 from 8B cells, CRISPR/Cas9 technology (Origene) was applied. The extend of reduction of IL-6 in the supernatant was analysed using Legendplex with an FC500 instrument.

Effect of nicotinamide mononucleotide on inhibiting senescent Mφ induction by 8B supernatant

Magnetic-sorted splenic $F4/80^+$ cells were cultured with the 8B supernatant for 14 days. During culture, 1 mM nicotinamide mononucleotide (NMN) or saline was added three times/week; then, an SA-b-Gal assay was performed.

Effect of NMN on inhibition of Arginase-1 expression

Whole splenocytes from C57BL/6 mice were cultured with the 8B supernatant for 7 days. During culture, 1 mM NMN or saline were added on day 0, 1, 3, and 6. On day 7, resulting cells were harvested and stained with anti-CD11b antibody. After twice washing, cells were fixed in 4% paraformaldehyde. After permeabilising the cells using Intracellular Staining Permeabilization Wash Buffer (Biolegend), they were stained with anti-Arginase 1 monoclonal antibody (clone A1exF5, Thermo Fisher Scientific). Cells were analysed with BD FACSCelesta™ (BD Biosciences); data were analysed with FlowJo software.

Analysis of Mφ's immune activating capacity

Whole splenocytes from C57BL/6 mice were cultured in M-CSF (20 ng/mL) or in 8B conditioned medium as described above with 1 mM of NMN or saline for 7 days. NMN or saline was added to the culture at day 1, 3, and 6. Resulting adherent macrophages were used. T cells were collected from the spleens of BALB/c mice by magnetic cell sorting using anti-Thy1.2 MACS beads (Miltenyi Biotec). Collected BALB/c T cells were labelled with CFSE and then co-cultured with collected macrophages (responder/stimulator ratio = 2) for 4 days. T cell proliferation was evaluated by measuring the reduction in CFSE fluorescence by flow cytometry.

Effect of NMN on 8B-transplanted mice survival

C57BL/6 mice were transplanted with 1000 8B cells in the brain. The mice received 10 mg NMN or saline by intraperitoneal injection three times/week. The survival time of the mice was determined.

Effect of NMN on tumour-initiation and mice survival in CT26-transplanted animals

5×10^4 CT26 cells were subcutaneously injected into syngeneic immunocompetent BALB/c mice. The mice received 10 mg NMN or saline by intraperitoneal injection three times/week. Tumour initiation was evaluated using ocular inspection and palpation. Tumour volume was calculated by the following formula: $((\text{short diameter})^2 \times (\text{long diameter}))/2$

Gene expression analysis in human glioblastoma tissue

Gene expression analysis of human glioblastoma tissue and normal brain tissue were performed using GEPIA, a web server for cancer and normal gene expression profiling [18].

Statistics

JMP software (JMP Version 16.0.0, SAS Institute Inc.) was used for statistical analysis. Data represent mean ± SEM. The Student's *t*-test (unpaired, two-tailed) or Tukey's honest significant difference (HSD) test was used to test for statistically significant differences. Mouse survival was analysed by Kaplan-Meier survival curves with the Log-rank test. When more than three experimental groups were performed, the results of the analysis were adjusted by Bonferroni correction.

Results

Host immunodeficiency level does not affect 8B tumour formation, whereas 9G tumour formation is affected

To analyse the requirement for tumour initiation followed by stable growth in immunocompetent individuals, we used the mouse inducible glioblastoma cell lines 8B and 9G [15], which were previously established by overexpression of an oncogenic H-Ras^{L61} in p53-deficient neural stem cells on the C57BL/6 background. As Hide et al. [15] previously described, 8B and 9G lines showed similar growth profiles *in vitro* (ref. 15 and Fig. 1A). However, these two lines showed a different phenotype when the cells were inoculated into nude mouse brains; 8B cells stably grew in the inoculated mouse brain and eventually killed the mice, but 9G cells did not stably grow in the brain and all mice survived during the observation period [15]. Hide et al. had concluded the difference in tumorigenicity between 8B and 9G was tumour-cell-intrinsic. However, we wondered whether this difference in tumorigenicity of both cell lines was not only due to cell-intrinsic properties but also to active immunity. To address this, we further performed experiments using C57BL/6 mice which are immunocompetent and syngeneic to the 8B and 9G. In the C57BL/6 mice, 85% of the animals did not survive inoculation with 8B cells while after injection with 9G cells only ~40% of the mice died ($P = 0.00333$, Log-rank test) (Fig. 1B), which are similar data as previously observed using nude mice [15]. Next, we tested tumour-formation of 8B and 9G cells in severe immunodeficient NOD/SCID mice that have a deficiency in T and B cells and reduced macrophage (Mφ) and NK cell activity. Interestingly, all the NOD/SCID mice died not only after 8B tumour cell inoculation but also due to 9G cell tumour formation, albeit at a slower pace as it took nearly double the time for all mice to be dead (NS; $P \geq 0.0083$ (i.e., 0.05/6), Bonferroni correction, Log-rank test) (Fig. 1B). These results suggested that the tumour-initiation and following stable growth were regulated at least partly by host immunity. Similar to the observation by Quintana et al. [14], the tumour forming capacity of 8B and 9G cells was significantly influenced by immune deficiency at the host level.

Although CD133 is a well-known marker of glioblastoma-initiating cells [19] [7], its expression was detected neither on 8B nor 9G (Supplementary Fig. 1).

Mφs have overwhelmingly infiltrated the 8B- and 9G-tumour microenvironment

Tumour cells arise from normal cells whose genome has been genetically/epigenetically altered by various factors, such as mutagens or radiation, and are characterised by their ability to multiply indefinitely. Many tumour cells proliferate indefinitely in culture dishes. However, not all such tumour cells form tumours *in vivo*. As shown in Fig. 1A, 8B and 9G cells grow stably in culture dishes. However, the situation is different *in vivo*: 9G cells grow stably in immunocompetent individuals, but have difficulty growing in immunocompetent individuals. On the other hand, 8B cells continue to proliferate stably in immunocompromised individuals and even in immunocompetent individuals and eventually kill the individual. These results suggest that whether *de novo* tumour cells eventually lead to stable tumour formation in an individual may be influenced by immunological factors in that individual. We therefore analysed why potential tumour-initiating cells such as 8B cells stably form tumours in immunocompetent individuals, but not 9G cells, focusing on differences in the interaction of 8B and 9G with immune cells.

To analyse what interaction between potential tumour initiating/forming cells and immune cells in the early period of tumour stable formation, we injected only a thousand 8B or 9G glioblastoma cells orthotopically as a potentially tumour-initiating population into syngeneic immunocompetent animals. We analysed what kind of immune cells infiltrated the tumour area. Immunohistochemical analysis showed a remarkable infiltration of $CD11b^+$, $F4/80^+$ cells, a small population of $CD11c^+$ cells; as well as a small number of $CD3^+$ T cells and several $CD19^+$ cells or $Ly6g^+$ cells were observed in both 8B and 9G tumour tissues (Supplementary Fig. 2). This result in the glioblastoma model suggests that immune cell infiltration into the tumour occurs and interaction is likely.

In these glioma tissues, $CD11b^+$ cells overwhelmingly infiltrated. In the brain, not only macrophages but also microglia are known as CD11b expressing cells [20], so we questioned whether microglia had infiltrated into the glioblastoma tissues. To elucidate this, we stained the tumour tissue with the microglia specific P2RY12 antibody [21] [22] to distinguish microglia from peripherally infiltrating Mφs. Co-staining using P2RY12 and F4/80 antibodies indicated that $F4/80^+$ Mφs, rather than $P2RY12^+$ microglia, selectively infiltrated into the glioblastoma tissue (Supplementary Fig. 3A and 3B). Therefore, we hereafter focused on peripherally infiltrating Mφs rather than microglia for further *in vitro* experiments.

Mφ depletion prolong survival of 8B inoculated mouse

To define the importance of Mφs in tumour initiation followed by stable growth in immunocompetent mice, we depleted Mφs *in vivo*. In mouse glioblastomas, the timing of tumour initiation and stable growth itself is difficult to monitor and was therefore assessed by mouse death.

We observed survival/death of 8B-transplanted mice for a long enough period to be able to evaluate the Mφ contribution in tumour-initiation followed by stable growth: in mice orthotopically implanted with 8B, the time to final death was 266 days (N=30) (Fig. 1A). Therefore, day 365 was set as a sufficient period to observe the final survival/death of mice transplanted with 8B, and the contribution of Mφ in tumour development was assessed with the mice alive or dead at 365 days.

Since the F4/80 antibody do not deplete $F4/80^+$ cells in vivo, we instead administered an anti-CD11b antibody (M1/70 proven for $CD11b^+$ cells depletion [23]), as the majority of $F4/80^+$ cells are CD11b positive (data not shown). We further used the RB6-8C5 (anti-Gr-1) antibody [24] which depletes other types of myeloid lineage cells mainly granulocytes, and rat IgG as experimental controls. In the Mφ-depleted group (anti-CD11b group), the ratio of mice alive tended to be higher, although not significantly so, than in the control IgG group (Chi-square test (Pearson), $\chi 2$ (1) =4.286, p=0.0384) (The p values <0.05/3=0.0167 (Bonferroni correction) was considered as statistically significant) (Supplementary Fig. 4A and B), suggesting that the role of Mφs was important during the tumour-initiation and following growth.

8B cells made resistant to macrophage proliferation

To analyse whether tumour cells regulate the activity of immune cells, we performed a co-culture experiment of tumour cells and spleen cells. Splenocytes include various kinds of immune cells, including macrophages. In the analysis, Mφs depicted by $F4/80^+$ or $CD11b^+$ efficiently proliferated in the 9G co-culture, although their proliferation was less in the 8B co-culture compared with the 9G co-culture (Fig. 2A). The reduced proliferation was also observed when tumour supernatant was used instead of tumour cells (Data not shown). These results suggest that one or more soluble factor(s) secreted by these tumour cells affect Mφ proliferation.

After 14 days culturing $F4/80^+$ cells with 8B or 9G tumour cell supernatant (8B-Mφ or 9G-Mφ, respectively), the morphology of the resulting Mφs showed clear differences (Fig. 2B). A large proportion of 8B-Mφs showed a flattened and enlarged appearance compared to the 9G-Mφs (Fig. 2B). This difference in cell size was also observed by flow cytometry (Fig. 2C).

We also performed morphological analysis of the Mφs after splenocytes were cultured with the respective tumour supernatants. The Mφs those that did not proliferate (Fig. 2D, gate) and those that did proliferate and expressed Ly6c (Fig. 2D, gate) appeared round-shape, just like the senescent cells in both the 8B-sup and 9G-sup cultures. Interestingly, the CFSE-reduced, i.e. proliferated, Ly6c-negative Mφ populations of 9G-sup cultures (Fig. 2D, gate III) clearly had pseudopodia, suggesting that these Mφ were not in the senescent state. On the other hand, the corresponding Mφ population in 8B-sup cultures showed a round shape (Fig. 2D, gate III), suggesting that they may have entered the senescence-like state after proliferation. These morphological observations indicate that some fractions of 9G-Mφs were in a non-senescence-like state, but most fractions of 8B-Mφs were in a senescence-like state.

8B induced Mφs into a senescence-like state

These observations suggested that the appearance of Mφs induced by 8B tumours was similar to that of cells in a senescence-like state. Therefore, we explored whether the Mφs were in such a state using a senescence-associated β-galactosidase (SA-b-Gal) assay. Flattened and enlarged Mφs showed β-galactosidase activity. The proportion of β-galactosidase-positive Mφs was about 1.6-times larger in 8B-Mφs than in 9G-Mφs (Fig. 2E). Additionally, we performed SA-b-Gal staining in brain tumours that were

established after injection of 8B and 9G cells. Positive b-gal activity was observed around the tumour region in the 8B-transplanted brain, whereas no significant positive staining was detected in the 9G-transplanted brain (Fig. 2F). Most of the cells showing SA-β-gal activity (senescent cells) in the 8B tumour were, although not all, F4/80 positive (Fig. 2G). The proportion of the SA-β-Gal positive area within the $F4/80^+$ population was approximately 1.8-fold higher in 8B than in 9G tumours (Fig. 2H). Furthermore, we analysed the series of cellular senescence-related genes expression in Mφs. The analysis revealed that 8B-Mφs highly expressed *p21* and *Glb1* (Fig. 2I) compared to 9G-Mφs among six tested genes which are known to correlate with cellular senescence [25].

Historically, many classifications of Mφs have been proposed [26], the major being M1/M2 [27]. Tumour-associated Mφs are commonly classified as M2 Mφs [26] [28]. Although 8B cells with tumour-initiating capacity are expected to induce Mφs with an M2 phenotype, 8B-Mφs did neither express most of the M2-Mφs-related genes such as *Irf4* or *Retnla*, except for *Arg1* (Fig. 2J), nor did 8B-Mφs M1-related genes. Furthermore, 9G-Mφs do also not express the typical gene profile to fit the M1/M2 classification (Fig. 2J). Thus, these data indicated that 8B- and 9G-Mφs cannot be classified as M1 or M2 based on their gene expression pattern.

8B tumour infiltrating $CD3^+$ T cells downregulate CD3ζ

Despite the infiltration of $CD3^+$ T cells in the 8B-tumour environment in immunocompetent mice (Supplementary Fig. 2), tumour growth was persistent (Fig. 1B), suggesting suppression of T cell activity in the tumour tissue. Arginase-1 is known to be a strong immunosuppressive molecule that downregulates the expression of CD3ζ, a key intracellular molecule in T cell signalling, and inducing hyporesponsiveness of these cells [29]. We observed an expression of *Arg1* in 8B-Mφs but not in 9G-Mφs (Fig. 2J). When we analysed CD3ζ expression in T cells from 8B and whole splenocyte co-cultures, including T cells and macrophages, 17A2 antibody staining positive $CD3\varepsilon/\gamma/\delta^+$ T cells, i.e. surface CD3 positive T cells lost their CD3ζ expression. In contrast, surface $CD3^+$ T cells retained CD3ζ expression in the 9G co-culture (Fig. 2K). *In vivo* analysis revealed that CD3ζ expression was observed in ~75% of surface $CD3^+$ T cells in 9G tumours, but only in ~30% of surface $CD3^+$ cells in 8B-tumour tissue (Fig. 2L). To further understand the activity of tumour-specific T cells, we analysed T cells harvested from 8B tumour-immunized C57BL/6 mice. As expected, IFN-γ production was approximately ten-fold lower in CD3ζ-negative T cells compared to CD3ζ-positive T cells (Fig. 2M). Thus, although T cells infiltrated heavily into the 8B tumour, most of these T cells lost their CD3ζ expression and suggested became dysfunctional. It is therefore suggested that 8B tumours induce dysfunction of infiltrating T cells by downregulating their CD3ζ expression and that resulted in the development of tumours in immunocompetent mice.

8B-derived IL-6 induce Mφs into a senescence-like state

Next, we focused on the unknown factor(s) that induced the senescence-like phenotype of Mφs. We analysed the tumour culture supernatant by cytokine/chemokine array and found interleukin-6 (IL-6),

Ccl5, Cxcl1, and Cxcl10 were selectively secreted by 8B cells, where Ccl2 was secreted at a 2x higher amounts (Fig. 3A). Notably, some of these factors, such as IL-6 and Cxcl1, are known to be senescence-related cytokines/chemokines [30] [31]. To identify which of these cytokine(s) is/are important for inducing the senescence-like state in Mφs, we cultured splenocytes in the presence of the cytokines secreted by 8B or after withdrawal of each individual cytokine/chemokine from the five candidates (Fig. 3B). Accelerated senescence induction in Mφs was observed in the presence of the five cytokines compared to in their absence. After withdrawal of either Ccl2 or IL-6, the numbers of b-galactosidase-positive Mφs were reduced. Notably, SA-b-Gal-positive Mφs were reduced to the same level as in the negative control by withdrawing IL-6. This result, together with the observation that 9G sup also contained Ccl2, suggests that IL-6 is the responsible factor for inducing Mφs into the senescence-like state.

The p38 MAPK signalling pathway is responsible for IL-6 secretion in 8B

Next, we attempted to identify the signalling pathway that induces selective expression of IL-6 in 8B cells. We used the following inhibitors: U0126 (MEK1/2 inhibitor), LY294002 (PI3K inhibitor), BAY117082 (NFkB inhibitor), SB203580 (p38 inhibitor), SP600125 (JNK inhibitor), and PD0325901 (MEK1/2 inhibitor). Because BAY117082 was strongly cytotoxic for 8B at low concentrations (even at 1 mM), it was difficult to use it in this assay (Supplementary Fig. 5A). Although all inhibitors were relatively more toxic for the cells than vehicle alone, IL-6 secretion was maintained by MEK1/2 inhibition by U0126 and PI3K inhibition by LY294002. In contrast, JNK inhibition by SP600125 and MEK1/2 inhibition by PD0325901strikingly up-regulated IL-6 secretion, whereas p38 inhibition by SB203580 led to decrease of IL-6 secretion (Supplementary Fig. 5B); thus, p38 MAPK signalling is important for IL-6 secretion in 8B cells.

As described above, both the IL-6 producer 8B and the non-producer 9G originate from the same cell line [15]. The cause of their different IL-6 secretion is unclear. Ohsawa et al. [32] reported that constitutive activation of Ras and mitochondrial dysfunction in drosophila cells resulted in *upd* (an ortholog of human/mouse IL-6) secretion and tumour formation *in vivo*. As 8B and 9G cells both bear constitutive active Ras, we speculated that a difference in their respective mitochondrial dysfunction results in the different IL-6 production. As mitochondrial dysfunction results in the accumulation of reactive oxygen species (ROS) within cells, we compared ROS accumulation in 8B and 9G cells. In the presence of excess amounts of *N*-acetylcysteine (NAC) (5000 μM), ROS levels were detected almost equally in 8B and 9G. In contrast, higher ROS levels were recorded in 8B in the presence of 500 μM NAC or in the absence of NAC. (Supplementary Fig. 5C). Considering that elevated ROS levels induce p38 activation [33], activation of the ROS-p38 axis was suggested to be the possible mechanism of selective IL-6 secretion in 8B in relation to 9G.

8B derived IL-6, a senescence inducible factor of Mφs, is one of the factors responsible for tumorigenesis in immunocompetent C57BL/6 mice

Next, we focused on the impact of IL-6 secreted by 8B on senescence induction in Mφs and tumour-forming capacity *in vivo*. We created 8B-IL-6-knockout cells (8B-IL-6-KO) by CRISPR/Cas9 technology as well as mock transfectants with scrambled guide-RNA transfected 8B cells (8B-mock) (Fig. 3C). Both cell lines proliferated comparably *in vitro* (Fig. 3D). The flattened and enlarged appearance of Mφs was observed when cells were cultured in 8B-mock supernatant culture, whereas Mφs with pseudopodia were observed in the 8B-IL-6-KO supernatant culture (Fig. 3E). In 8B-IL-6-KO-Mφs, expression of *Glb1*, *p16*, *p19*, *p21*, and *Arg1* was lower than in 8B-mock-Mφs (Fig. 3F). Thus, Mφs induced by the 8B-IL-6-KO supernatant lost their senescent features, suggesting that IL-6 secreted by 8B cells is indeed the factor responsible for senescence induction in Mφs.

We further analysed the impact of IL-6 on tumorigenicity (Fig. 3G). 8B-IL-6-KO cells, as well as 8B-mock cells, exerted tumorigenicity in NOD/SCID mice, and all mice died by 200 days after tumour inoculation. Interestingly, only 8B-mock cells still exerted tumorigenicity in immunocompetent C57BL/6 mice, and almost all the mice died in a similar time course as the NOD/SCID mice. In contrast, 8B-IL-6-KO cells showed remarkable reduced tumorigenicity in C57BL/6 mice as about 60% of the mice survived more than 400 days after the inoculation of 8B-IL-6-KO cells. This indicates that tumour cells that were not secreting IL-6 were not capable to form a tumour in immunocompetent mice, although they could do so in immunodeficient mice. In contrast, IL-6 secretion by tumour cells allowed tumour formation not only in immunodeficient mice but even in immunocompetent mice. Thus, IL-6 secretion by tumour cells defines their capacity of tumour-initiation and following growth in immunocompetent mice in this orthotopic glioblastoma transplantation model.

Senescence-like Mφs induced by 8B express high levels of CD38, and supplementation with its substrate, nicotinamide mononucleotide, suppresses the Mφs go into a senescence-like state

To identify a surface protein that was selectively expressed in senescence-like Mφs, we examined a series of cell surface molecules by flowcytometry. From the experiments, we found that 8B-sup induced senescence-like Mφs expressed CD38 at a higher level compared to 9G-sup induced Mφs (Fig. 4A and Supplementary Fig. 6). In addition, more than 70% of $F4/80^+$ cells expressed CD38 in 8B-tumours. In contrast, CD38 expression was detected only on ~25% of the $F4/80^+$ cells in 9G-tumours (Fig. 4B). CD38 is a membrane-bound multifunctional protein with NADase activity that hydrolyzes NAD^+ to nicotinamide and cyclo-ADP-ribose, and its expression is known to increase with age and aging [34]. A recent analysis revealed that CD38 is the main enzyme involved in NAD precursor nicotinamide mononucleotide (NMN) degradation *in vivo* [35]. As the NAD level is reduced with age and is involved in age-related metabolic decline [35], exogenously supplying NAD may prevent senescence. Therefore, we predicted that adding NMN would cancel the senescence phenotype of Mφs and change the tumour microenvironment into an anti-tumorigenic state. We found that the addition of NMN to the 8B-Mφ culture resulted in Mφs with pseudopodia (Fig. 4C). Furthermore, the number of SA-b-Gal-positive senescence-like Mφs was reduced after addition of NMN (Fig. 4C), and Arginase-1 expression in 8B-Mφs cultured in the presence of NMN showed a three-fold reduction of Arginase-1 expression compared to the control culture (Fig. 4D).

Possible existence of senescent Mφ in human glioblastoma tissue

Several gene expressions in human glioblastoma tissues were analysed using GEPIA, a web server for cancer and normal gene expression profiling and interactive analyses based on TCGA and GTEx data (Supplementary Fig. 7A and B) [18]. High expression of *CD11B* and *CD14*, those mainly observed in monocytes and macrophage, was identified in human glioblastoma tissues than in normal brain tissues, suggesting a macrophage infiltration in glioblastoma tissue. *IL-6*, defined as Mφ senescence inducible cytokine in the mouse glioblastoma model (Fig. 3A-G), and *CD38,* that detected in senescent Mφs (Fig. 4A), were also detected with higher levels in glioblastoma tissues than in normal tissues. These results suggested a possibility that senescent Mφ were infiltrated in human glioblastoma tissues. Further, pairwise Pearson correlation between *CD38* and *ARG1* expression in human glioblastoma tissues were analysed using GEPIA. There was a significant correlation between them, suggesting a possibility of senescent Mφ expressing *ARG1*.

Exogenous supplementation of NMN converts Mφs from an immunosuppressive to an immunogenic state

We analysed whether the addition of NMN contributes to the improvement of immune activating capacity of senescence-like macrophages. The addition of NMN to the 8B-Mφ culture resulted in Mφs with pseudopodia, resembling dendrites of dendritic cells (Fig. 4C). From this result, we speculated NMN treatment might improve the immune activating capacity of 8B-Mφ. Therefore, we further measured the effect of NMN treatment on the immune activating capacity of 8B-Mφs by using an allogeneic T cell response assay as one of immune activating capacity evaluation (Fig. 4E). Although $CD8^+$ T cells proliferated efficiently in an M-CSF induced Mφ co-culture, their proliferation ratio was ~3-fold reduced in saline-treated 8B-Mφ co-cultures, to the same extend as the NMN-treated culture. $CD4^+$ T cells showed a ~2-fold reduced proliferation in the saline-treated 8B-Mφ co-culture compared to the M-CSF induced Mφ co-culture. Notably, $CD4^+$ T cell proliferation in the NMN-treated 8B-Mφ co-culture was restored to the level as was obtained in the M-CSF induced Mφ co-culture. Thus, NMN treatment improves the immune activating capacity of 8B-Mφs.

NMN supplementation therapy prevents tumour initiation in 8B-inoculated immunocompetent mice

Finally, we analysed the effectiveness of NMN treatment in preventing 8B-tumour initiation using the orthotopic tumour transplantation model in immunocompetent C57BL/6 mice (Fig. 4F). In the saline treated group, ~70% of mice showed tumour initiation and died as a result. In contrast, in the NMN treated group, tumour initiation was observed in only ~20% of mice, and survival was improved compared to that in the saline group ($P = 0.076$, Log-rank test).

In the glioblastoma orthotopic transplantation model, it is difficult to precisely determine the date of tumour initiation and formation. To examine the precise timing, we attempted to analyse subcutaneous tumour formation. However, 8B and 9G cells did not form any tumour when subcutaneously inoculated (data not shown). Therefore, we chose CT26 subcutaneous engraftable syngeneic tumour model to

analyse the effect of NMN on tumour formation. As the CT26 mouse colorectal cancer cells secrete IL-6[36], Mφ senescence induction via IL-6 in the tumour microenvironment is expected. We therefore injected CT26 cells subcutaneously into syngeneic BALB/c immunocompetent mice and evaluated the effect of NMN treatment on tumour formation. The NMN treatment significantly delayed the tumour initiation ($P < 0.05$, Log-rank test) (Fig. 4G) and efficiently inhibited the tumour growth (Fig. 4H). Collectively, these results suggested that NMN treatment suppressed the senescence of Mφs that induces T cell dysfunction by expressing Arginase-1, and eventually but temporarily, prevented tumour initiation in immunocompetent mice.

Discussion

Our understanding of the requirements and mechanisms allowing tumour-initiating cells to form tumours in immunocompetent individuals remains insufficient. In this study, a series of experiments showed that senescence in Mφs played a pivotal role in tumour-initiation in immunocompetent mice. One of the mechanisms is that tumour cell-derived IL-6 induces senescence of Mφ, which in turn induces T cell dysfunction through the expression of Arginase-1 by their macrophages, enabling tumour development even in immunocompetent animals. These results suggest that tumour cells that have the capacity to induce macrophage senescence could be authentic tumour-initiating cells in immunocompetent animals.

It is known that cellular senescence affects immune responses, including both stimulation and suppression [37] [38] [39]. In the radiation-inducing osteosarcoma mouse model, tumour cells go into senescence and express SASP factors, including IL-6. In this model, IL-6 plays an immune-activation role by recruiting NK cells [38]. In another model, senescent stromal cells express Ccl2, which plays an immunosuppressive role by recruiting myeloid-derived suppressor cells that inhibit tumour clearance by NK cells [39]. In the current study, we propose a new mechanism whereby Mφ-senescence-like phenotypes driven by tumour cell-derived IL-6 induce immunosuppression that eventually leads to tumour initiation in immunocompetent individuals. Moreover, preventing senescence by the exogenous administration of a metabolic substrate suppressed tumour initiation *in vivo*. This finding clearly indicates that Mφ senescence can contribute to tumour initiation.

8B tumour cells have infinite cell division activity with continuous IL-6 production, leading to immunosuppression. Such cells achieved tumour-initiation cell-autonomously even in immunocompetent individuals. Therefore, we considered that having both features in one cell is one of the requirements for autonomous tumour-initiation by cells in immunocompetent individuals. From another perspective, our results give consideration to the simultaneous existence of infinitely proliferating tumour cells and an immunosuppressive environment that also is a condition that can lead to tumour-initiation in immunocompetent individuals. Patients with inflammatory bowel disease (IBD) are susceptible to colorectal cancer [40], and this may be an example of the concept. Abundant reactive oxygen species (ROS) exist in inflammatory environments [41] and can cause genetic damage [41], generating cells that divide infinitely. IL-6 is also present in the same environment [42]. Thus, the bowel environment of patients with IBD seems to correspond to the tumour-initiation requirement, even if the patient has a

healthy (albeit overactive) immune system. This may explain why patients with IBD are more susceptible to colorectal cancer.

We cannot exclude the possibility of other tumour-initiation mechanisms that may exist depending on the individual organ in immunocompetent individuals; in fact, subcutaneous inoculation of 8B cells (1000 cells; this number is sufficient for tumour formation in the brain) did not form a tumour mass (data not shown) in the skin.

As we mentioned above, the contribution of cellular senescence to cancer remains controversial. However, the addition of a metabolic substrate, NMN, which is reduced during senescence, inhibited the production of the immunosuppressive molecule Arginase-1 in Mφs, improving their T cell stimulating capacity towards $CD4^+$ T cells (Fig. 4E). These observations indicate that senescence, at least in Mφs, contributed to tumour initiation. Therefore, Mφ senescence regulating therapy using the metabolism improving drug NMN that is based on the mechanisms of immunosuppression cancellation and immuno-reactivation could be a promising novel cancer therapy.

Conclusion

In this study, we found that the tumour cells that are secreting IL-6 did allow tumour formation in immunocompetent animals by inducing senescence of macrophages. I.e., That means the tumour cells which have such phenotypes is authentic tumour-initiating cells in immunocompetent animals. Further, i*n vivo* administration of NMN prolonged the tumour free duration and survival in IL-6 expressing tumour inoculated immunocompetent mouse. We speculate that NMN administration would have inhibited Mφ senescence and would have induced immunogenicity of the tumour microenvironment at the moment that a tumour was "just initiated". This is a time point where only a small number of tumour cells and surrounding Mφs are present at the same location. Thus, for clinical application, NMN administration should be expected to suppress *de novo* tumour-initiation including metastasis suppression and could be applied after primary tumour resection. Therefore, this newly defined tumour-initiation mechanism in immunocompetent individuals will help to construct a novel strategy for cancer therapy.

Abbreviations

8B-IL-6-KO 8B-IL-6-knockout

8B-mock scrambled guide-RNA transfected 8B cells

IBD inflammatory bowel disease

Mφ macrophage

NAD nicotinamide adenine dinucleotide

NMN nicotinamide mononucleotide

ROS reactive oxygen species

SA-b-Gal senescence-associated β-galactosidase

Declarations

Ethics approval and consent to participate

All animal procedures were approved by the Hokkaido University Animal Care Committee (Approval number: 20-0182).

Consent for publication

Not applicable.

Availability of data and material

Not applicable.

Competing interests

The authors have declared that no conflict of interest exists.

Funding

This study was supported in part by research grants from the Ministry of Education, Culture, Sports, Science and Technology of Japan (HW and KS). This work was also supported in part by AMED under Grant Number 19bm0404028h0002 (KS), 19ck0106262h0003 (KS), the Kato Memorial Bioscience Foundation (HW), Suhara memorial foundation (HW), The Akiyama life science foundation (HW), Friends of Leukemia Research Fund (HW), and The Mitsubishi Foundation (KS).

Authors’ contributions

HW, and KS designed the study. HW wrote the initial draft of the manuscript. HW, RO, and TM contributed to acquisition of data. HW, RO, TM, TK and KS analysed and interpreted the data and assisted in the preparation of the manuscript. WG assisted in the preparation and writing of the manuscript. All authors approved the final version of the manuscript.

Acknowledgments

We would like to thank Dr. Muhammad Baghdadi for useful discussions. We gratefully acknowledge the technical assistance of Ms. Nanami Eguchi, Ms. Misuho Ito, Mr. Rei Kawashima, Ms. Chie Kusama, Ms. Ayano Yamauchi, and Ms. Rei Okabe.

Authors' information

Not applicable.

References

1. Meacham CE, Morrison SJ: Tumour heterogeneity and cancer cell plasticity. *Nature* 2013, 501(7467):328-337.
2. Steinbichler TB, Dudas J, Skvortsov S, Ganswindt U, Riechelmann H, Skvortsova, Il: Therapy resistance mediated by cancer stem cells. *Semin Cancer Biol* 2018, 53:156-167.
3. Plaks V, Kong N, Werb Z: The cancer stem cell niche: how essential is the niche in regulating stemness of tumor cells? *Cell Stem Cell* 2015, 16(3):225-238.
4. Peitzsch C, Tyutyunnykova A, Pantel K, Dubrovska A: Cancer stem cells: The root of tumor recurrence and metastases. *Semin Cancer Biol* 2017, 44:10-24.
5. Frank NY, Schatton T, Frank MH: The therapeutic promise of the cancer stem cell concept. *J Clin Invest* 2010, 120(1):41-50.
6. Qiu H, Fang X, Luo Q, Ouyang G: Cancer stem cells: a potential target for cancer therapy. *Cell Mol Life Sci* 2015, 72(18):3411-3424.
7. Chen K, Huang YH, Chen JL: Understanding and targeting cancer stem cells: therapeutic implications and challenges. *Acta Pharmacol Sin* 2013, 34(6):732-740.
8. Tirino V, Desiderio V, Paino F, De Rosa A, Papaccio F, La Noce M, Laino L, De Francesco F, Papaccio G: Cancer stem cells in solid tumors: an overview and new approaches for their isolation and characterization. *FASEB J* 2013, 27(1):13-24.
9. Sherry MM, Reeves A, Wu JLK, Cochran BH: STAT3 Is Required for Proliferation and Maintenance of Multipotency in Glioblastoma Stem Cells. *Stem Cells* 2009, 27(10):2383-2392.
10. Lee TKW, Castilho A, Cheung VCH, Tang KH, Ma S, Irene OLN: CD24(+) Liver Tumor-Initiating Cells Drive Self-Renewal and Tumor Initiation through STAT3-Mediated NANOG Regulation. *Cell Stem Cell* 2011, 9(1):50-63.
11. Lin L, Fuchs J, Li CL, Olson V, Bekaii-Saab T, Lin JY: STAT3 signaling pathway is necessary for cell survival and tumorsphere forming capacity in ALDH(+)/CD133(+) stem cell-like human colon cancer cells. *Biochem Biophys Res Commun* 2011, 416(3-4):246-251.
12. Dunn GP, Bruce AT, Ikeda H, Old LJ, Schreiber RD: Cancer immunoediting: from immunosurveillance to tumor escape. *Nat Immunol* 2002, 3(11):991-998.
13. Binnewies M, Roberts EW, Kersten K, Chan V, Fearon DF, Merad M, Coussens LM, Gabrilovich DI, Ostrand-Rosenberg S, Hedrick CC *et al*: Understanding the tumor immune microenvironment (TIME) for effective therapy. *Nat Med* 2018, 24(5):541-550.
14. Quintana E, Shackleton M, Sabel MS, Fullen DR, Johnson TM, Morrison SJ: Efficient tumour formation by single human melanoma cells. *Nature* 2008, 456(7222):593-U533.
15. Hide T, Takezaki T, Nakatani Y, Nakamura H, Kuratsu J, Kondo T: Sox11 prevents tumorigenesis of glioma-initiating cells by inducing neuronal differentiation. *Cancer Res* 2009, 69(20):7953-7959.

16. Debacq-Chainiaux F, Erusalimsky JD, Campisi J, Toussaint O: Protocols to detect senescence-associated beta-galactosidase (SA-beta gal) activity, a biomarker of senescent cells in culture and in vivo. *Nat Protoc* 2009, 4(12):1798-1806.
17. Riquelme P, Tomiuk S, Kammler A, Fandrich F, Schlitt HJ, Geissler EK, Hutchinson JA: IFN-gamma-induced iNOS Expression in Mouse Regulatory Macrophages Prolongs Allograft Survival in Fully Immunocompetent Recipients. *Molecular Therapy* 2013, 21(2):409-422.
18. Tang Z, Li C, Kang B, Gao G, Li C, Zhang Z: GEPIA: a web server for cancer and normal gene expression profiling and interactive analyses. *Nucleic Acids Res* 2017, 45(W1):W98-W102.
19. Neuzil J, Stantic M, Zobalova R, Chladova J, Wang X, Prochazka L, Dong L, Andera L, Ralph SJ: Tumour-initiating cells vs. cancer 'stem' cells and CD133: what's in the name? *Biochem Biophys Res Commun* 2007, 355(4):855-859.
20. Galatro TF, Holtman IR, Lerario AM, Vainchtein ID, Brouwer N, Sola PR, Veras MM, Pereira TF, Leite REP, Moller T *et al*: Transcriptomic analysis of purified human cortical microglia reveals age-associated changes. *Nat Neurosci* 2017, 20(8):1162-1171.
21. Lund H, Pieber M, Parsa R, Han J, Grommisch D, Ewing E, Kular L, Needhamsen M, Espinosa A, Nilsson E *et al*: Competitive repopulation of an empty microglial niche yields functionally distinct subsets of microglia-like cells. *Nat Commun* 2018, 9(1):4845.
22. Butovsky O, Jedrychowski MP, Moore CS, Cialic R, Lanser AJ, Gabriely G, Koeglsperger T, Dake B, Wu PM, Doykan CE *et al*: Identification of a unique TGF-beta-dependent molecular and functional signature in microglia. *Nat Neurosci* 2014, 17(1):131-143.
23. Ault KA, Springer TA: Cross-reaction of a rat-anti-mouse phagocyte-specific monoclonal antibody (anti-Mac-1) with human monocytes and natural killer cells. *J Immunol* 1981, 126(1):359-364.
24. Stoppacciaro A, Melani C, Parenza M, Mastracchio A, Bassi C, Baroni C, Parmiani G, Colombo MP: Regression of an Established Tumor Genetically-Modified to Release Granulocyte-Colony-Stimulating Factor Requires Granulocyte T-Cell Cooperation and T-Cell Produced Interferon-Gamma. *J Exp Med* 1993, 178(1):151-161.
25. Burton DGA, Krizhanovsky V: Physiological and pathological consequences of cellular senescence. *Cell Mol Life Sci* 2014, 71(22):4373-4386.
26. Mantovani A, Sozzani S, Locati M, Allavena P, Sica A: Macrophage polarization: tumor-associated macrophages as a paradigm for polarized M2 mononuclear phagocytes. *Trends Immunol* 2002, 23(11):549-555.
27. Mills CD: Anatomy of a discovery: m1 and m2 macrophages. *Front Immunol* 2015, 6:212.
28. Chanmee T, Ontong P, Konno K, Itano N: Tumor-Associated Macrophages as Major Players in the Tumor Microenvironment. *Cancers* 2014, 6(3):1670-1690.
29. Rodriguez PC, Quiceno DG, Zabaleta J, Ortiz B, Zea AH, Piazuelo MB, Delgado A, Correa P, Brayer J, Sotomayor EM *et al*: Arginase I production in the tumor microenvironment by mature myeloid cells inhibits T-cell receptor expression and antigen-specific T-cell responses. *Cancer Res* 2004, 64(16):5839-5849.

30. Kojima H, Inoue T, Kunimoto H, Nakajima K: IL-6-STAT3 signaling and premature senescence. *JAKSTAT* 2013, 2(4):e25763.
31. Kim EK, Moon S, Kim DK, Zhang XL, Kim J: CXCL1 induces senescence of cancer-associated fibroblasts via autocrine loops in oral squamous cell carcinoma. *Plos One* 2018, 13(1).
32. Ohsawa S, Sato Y, Enomoto M, Nakamura M, Betsumiya A, Igaki T: Mitochondrial defect drives non-autonomous tumour progression through Hippo signalling in Drosophila. *Nature* 2012, 490(7421):547-+.
33. Ito K, Hirao A, Arai F, Takubo K, Matsuoka S, Miyamoto K, Ohmura M, Naka K, Hosokawa K, Ikeda Y *et al*: Reactive oxygen species act through p38 MAPK to limit the lifespan of hematopoietic stem cells. *Nat Med* 2006, 12(4):446-451.
34. Chini EN, Chini CCS, Espindola Netto JM, de Oliveira GC, van Schooten W: The Pharmacology of CD38/NADase: An Emerging Target in Cancer and Diseases of Aging. *Trends Pharmacol Sci* 2018, 39(4):424-436.
35. Camacho-Pereira J, Tarrago MG, Chini CCS, Nin V, Escande C, Warner GM, Puranik AS, Schoon RA, Reid JM, Galina A *et al*: CD38 Dictates Age-Related NAD Decline and Mitochondrial Dysfunction through an SIRT3-Dependent Mechanism. *Cell Metab* 2016, 23(6):1127-1139.
36. Li J, Xu J, Yan X, Jin K, Li W, Zhang R: Targeting Interleukin-6 (IL-6) Sensitizes Anti-PD-L1 Treatment in a Colorectal Cancer Preclinical Model. *Med Sci Monit* 2018, 24:5501-5508.
37. Faget DV, Ren Q, Stewart SA: Unmasking senescence: context-dependent effects of SASP in cancer. *Nat Rev Cancer* 2019, 19(8):439-453.
38. Kansara M, Leong HS, Lin DM, Popkiss S, Pang P, Garsed DW, Walkley CR, Cullinane C, Ellul J, Haynes NM *et al*: Immune response to RB1-regulated senescence limits radiation-induced osteosarcoma formation. *J Clin Invest* 2013, 123(12):5351-5360.
39. Eggert T, Wolter K, Ji J, Ma C, Yevsa T, Klotz S, Medina-Echeverz J, Longerich T, Forgues M, Reisinger F *et al*: Distinct Functions of Senescence-Associated Immune Responses in Liver Tumor Surveillance and Tumor Progression. *Cancer Cell* 2016, 30(4):533-547.
40. Bernstein CN, Blanchard JF, Kliewer E, Wajda A: Cancer risk in patients with inflammatory bowel disease: a population-based study. *Cancer* 2001, 91(4):854-862.
41. Prasad S, Gupta SC, Tyagi AK: Reactive oxygen species (ROS) and cancer: Role of antioxidative nutraceuticals. *Cancer Lett* 2017, 387:95-105.
42. Stevens C, Walz G, Singaram C, Lipman ML, Zanker B, Muggia A, Antonioli D, Peppercorn MA, Strom TB: Tumor necrosis factor-alpha, interleukin-1 beta, and interleukin-6 expression in inflammatory bowel disease. *Dig Dis Sci* 1992, 37(6):818-826.

Figures

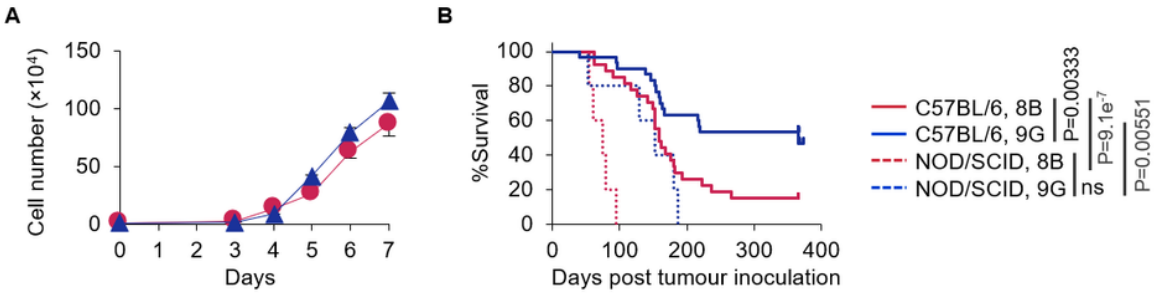

Figure 1

8B and 9G cells proliferated comparably *in vitro* but differently affected mouse survival based on the immunological background

A, Ten thousand 8B or 9G cells were seeded into a 96-well plate; the cell number was counted each day. Red circles indicate 8B; blue triangles indicate 9G. Error bars indicate the standard deviation from counts of triplicate wells in a single experiment. **B**, One thousand 8B or 9G cells were transplanted into C57BL/6 mouse brain (8B (red solid line) n = 30, 9G (blue solid line) n = 27) or NOD/SCID mouse brain (8B (red dotted line) n = 5, 9G (blue dotted line) n = 5); then, mouse survival was observed. Statistical analyses were performed using the log-lank test with Bonferroni correction. The p values <0.05/6=0.0083 (Bonferroni correction) were considered as statistically significant. NS, not significant.

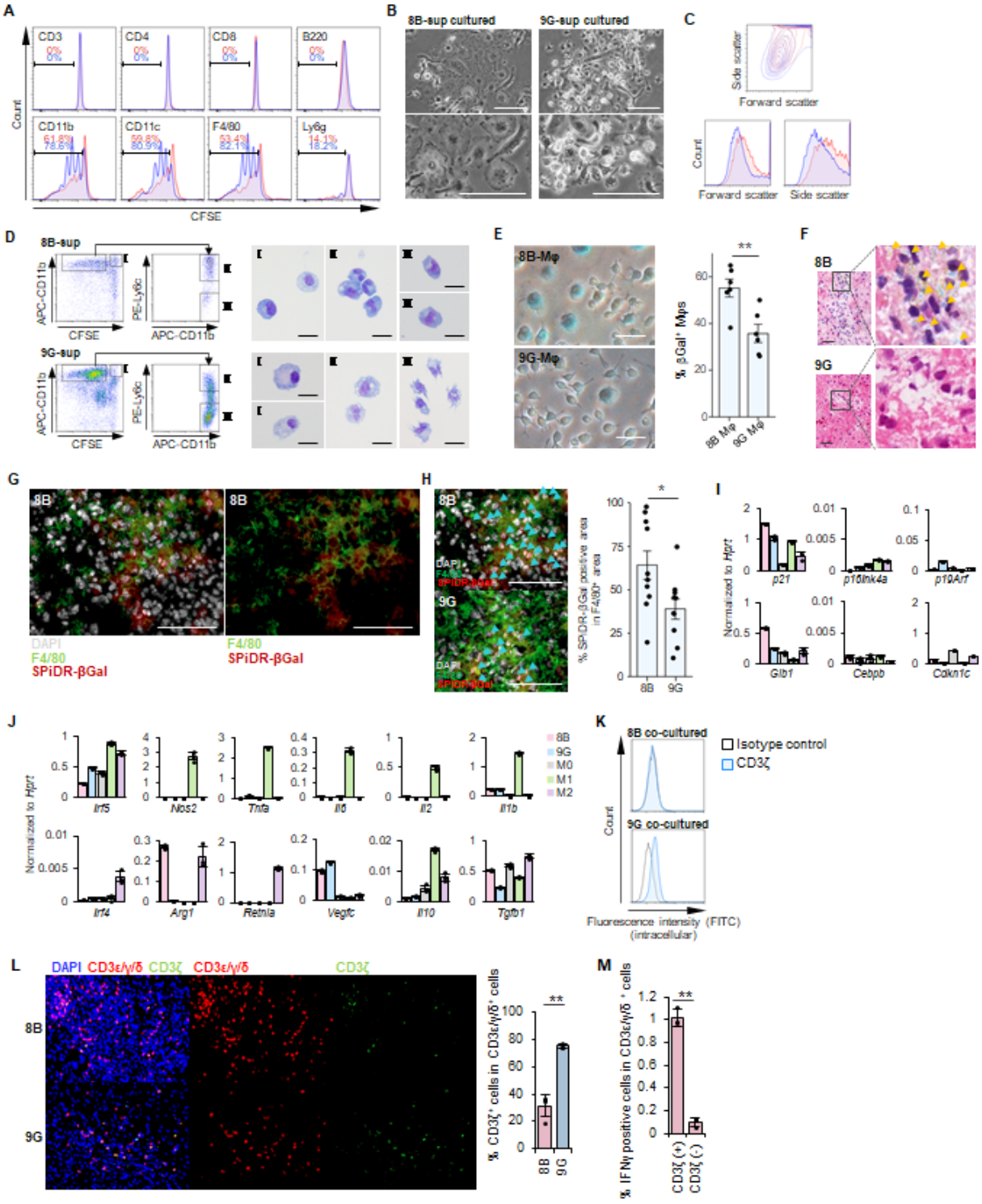

Figure 2

8B and 9G glioblastoma cells differently affected Mφs

A, Proliferation of immune cells in co-culture with 8B or 9G cells. Whole splenocytes from C57BL/6 mice were stained with carboxyfluorescein diacetate succinimidyl ester (CFSE) and then co-cultured with 8B or 9G for 5 days. The resulting cells were stained with the individual immune cell marker indicated in the

plots; CFSE reduction in each immune cell was flow cytometrically measured. The proliferation immune cell in 8B-co-cultured cells is shown in red histograms; 9G-co-cultured cells are shown in blue histograms. The % of proliferated immune cell in 8B-co-cultured cells is shown in red numbers; corresponding result of 9G-co-cultured cells are shown in blue numbers. **B**, Phase contrast images of generated Mφs by co-culture of splenic F4/80$^+$ cells and 8B or 9G supernatant. Bars; 50 mm. **C**, Whole splenocytes were cultured in 8B supernatant or 9G supernatant for 11 days. Generated cells were analysed by flow cytometry. Forward scatter and side scatter of generated CD11b$^+$ cells are shown. Red lines show 8B- 8B-cultured cells; blue lines show 9G-cultured cells. **D,** Morphological analysis of generated Mφs that proliferated in response to 8B or 9G supernatants. CFSE-labelled splenocytes were co-cultured with 8B or 9G for 4 days. Quiescent or proliferated CD11b$^+$ cells were sorted based on CFSE fluorescence reduction. Proliferated CD11b$^+$ cells were further subdivided into Ly6c-positive or Ly6c-negative fractions. Each fractionalized cell type was stained using a Diff-quick stain. Bars; 10 mm. **E**, Senescence-associated b-galactosidase (SA-b-Gal) assay was performed with generated Mφs in **C**. Mφs with flattened and hypertrophic round morphology, i.e. senescent cells, are stained blue. SA-b-Gal positive cells (at least 550) in six different views were counted; the proportion of positive cells was calculated. The bars indicate the mean (± SD). Each dot represents the SA-b-Gal % in each sample. **p < 0.01, Student's *t*-test. **F**, SA-b-Gal staining of the 8B or the 9G tumour-transplanted brain. Orange arrow heads indicate SA-b-Gal positive cells. Bars: 20 mm. **G** and **H**, SPiDR-βGal staining combined with F4/80 was applied on brain tissue seven days after mice were inoculated with 1000 cells 8B cells (**G** and **H**) or 9G cells (**H**). Sky-blue arrow heads in **H** indicated SPiDR-βGal staining positive cells. Percentages of SPiDR-βGal positive area within the F4/80$^+$ area in ten different views were calculated. The bars indicate the mean (± SD). Each dot represents the SPiDR-βGal positive area in F4/80$^+$ area in each sample. *p < 0.05, Student's *t*-test. Bars: 100 mm. **I**, Splenic F4/80$^+$ cells were cultured with 8B supernatant (pink) or 9G supernatant (sky blue). M0- (light grey), M1- (green), and M2- (purple) Mφs were also induced from splenic F4/80$^+$ Mφs as described by Riquelme et al. [17]. Gene expression related to cellular senescence in Mφs was analysed by RT-qPCR. The bars indicate the mean (+ SD). Each dot represents the relative value in normalized to *Hprt* of each sample. **J,** Splenic F4/80$^+$ cells were cultured with 8B- (pink) or 9G- (sky blue) supernatant for 7 days. M0- (right gray), M1- (green), and M2- (purple) Mφs were also induced from splenic F4/80$^+$ Mφs as described by Riquelme et al. [17]. Gene expression related to the Mφ M1/M2 classification was analysed by RT-qPCR. The bars indicate the mean (± SD). Each dot represents the relative value in normalized to *Hprt* of each sample. **K**, Whole splenocytes were co-cultured with 8B or 9G cells for 7 days. Intracellular CD3ζ expression in CD3$^+$ cells was analysed by flow cytometry. Blue lines indicate CD3ζ staining; black lines indicate isotype control staining. **L**, 8B or 9G cells were transplanted into the brain of C57BL/6 mice. After 28 days, the mouse brains were harvested. CD3ζ expression in CD3ε/γ/δ positive cells (it means whole CD3 positive T cells, here) in the tumour region was analysed by fluorescence immunohistochemistry. The proportion of CD3ζ$^+$ cells in CD3ε/γ/δ$^+$ cells was calculated based on cell number, and the averages and the standard deviations were calculated based on the results of four independent views. The bars indicate mean (± SD) of % CD3ζ$^+$ cells in CD3ε/γ/δ$^+$ cells. Each dot represents the % of CD3ζ$^+$ cells in CD3ε/γ/δ$^+$ cells in each sample. **p < 0.01, Student's *t*-test. **M**,

C57BL/6 mice were immunised with irradiated 8B cells once per week for 2 weeks. One week after the last immunisation, spleens were harvested. Whole splenocytes were co-cultured with intact tumour cells for 4 days; then, T cells were stimulated with PMA/ionomycin for 5 h in the presence of Golgistop® reagent; intracellular IFNγ expression was measured by flow cytometry. The proportion of $IFN\gamma^+$ cells among of $CD3\zeta^+$ or $CD3\zeta^-$ cells in the $CD3\varepsilon/\gamma/\delta^+$ population is shown in a bar graph. Error bars indicate standard deviation. Each dot represents the % of $IFN\gamma^+$ cells among of $CD3\zeta^+$ or $CD3\zeta^-$ cells in the $CD3\varepsilon/\gamma/\delta^+$ population in each sample. **p < 0.01, Student's *t*-test.

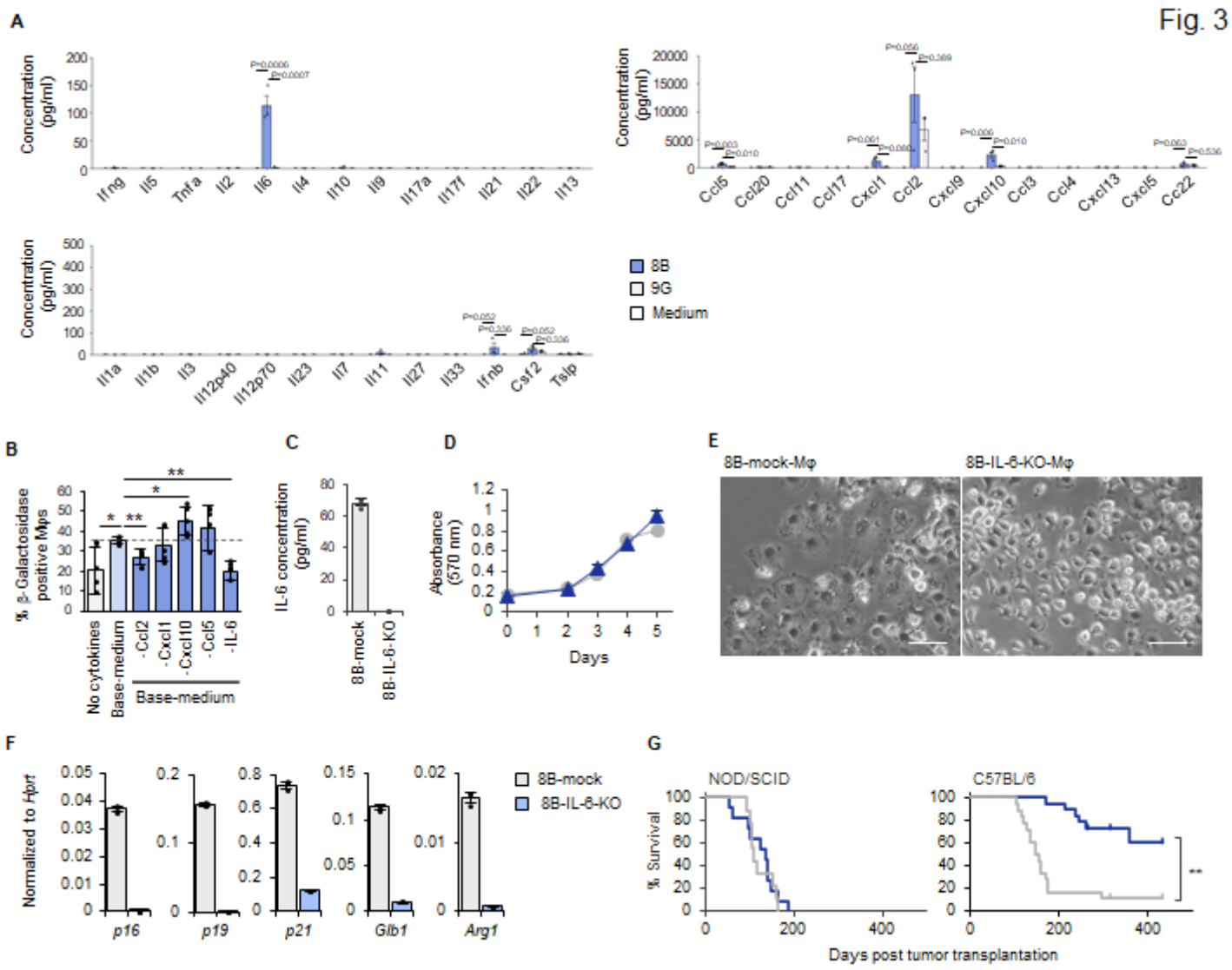

Figure 3

IL-6 secretion by glioblastoma cells defined the tumour-initiating capacity in immunocompetent animals

A, Cytokine secretion in 8B and 9G cells and medium was analysed by cytokine array. Each dot represents the cytokine concentration by three independent experiments. **B,** Identification of the responsible cytokine(s) secreted by 8B that induce Mφs into a senescence-like state. Splenocytes were cultured in medium containing recombinant cytokines corresponding to the types of cytokines secreted by 8B

identified in A. Glioma medium as used for 8B or 9G cultures was used to culture splenocytes. To support Mφs survival, M-CSF and IL-34were added to the glioma medium (Base-medium). To determine the factors responsible for Mφ senescence, Base-medium containing the major factors secreted by 8B, including Ccl2, Cxcl1, Cxcl10, Ccl5, and IL-6 (all factors) was used. Each factor from a pool of five cytokines were removed from the base-medium and splenocytes were cultured to analyse the requirement of each cytokine in the induction of senescence-like Mφs. The generated Mφs were analysed by SA-b-Gal assay. SA-b-Gal-positive cells in six different views were counted; the proportion of positive cells was calculated. The bars indicate the mean (± SD). Each dot represents the % of β-Galactosidase positive Mφs in each sample. *p < 0.05, **p < 0.01, Tukey-Kramer HSD test. **C**, The IL-6 gene was targeted in 8B cells by CRISPR/Cas9. Grey bar indicates 8B-mock; blue bar indicates 8B-IL-6-KO. **D**, Cell proliferation activity was measured daily by the MTT assay. 8B-mock and 8B-IL-6-KO proliferated comparably *in vitro*. The symbols indicate the mean (± SD). Grey circles indicate 8B-mock; navy triangles indicate 8B-IL-6-KO. **E,** Impact of 8B derived IL-6 on Mφs induction into a senescence-like state. Four-day culture supernatant of 8B-mock or 8B-IL-6-KO cells was used during splenic-F4/80^{+} cell culture. After 14 days, generated Mφs were observed by phase-contrast microscopy. Bars; 50 μm. **F,** Gene expression of generated Mφs prepared in C was analysed by RT-qPCR. The bars indicate the mean (± SD). Each dot represents the relative value in normalized to *Hprt* of each sample. **G,** One thousand 8B-mock or 8B-IL-6-KO cells were transplanted into NOD/SCID (8B-mock (grey) n = 9, 8B-IL-6-KO (navy) n = 11), or C57BL/6 mouse brain (8B-mock (grey) n = 18, 8B-IL-6-KO (navy) n = 19), and mouse survival was examined. **p < 0.01, log-lank test.

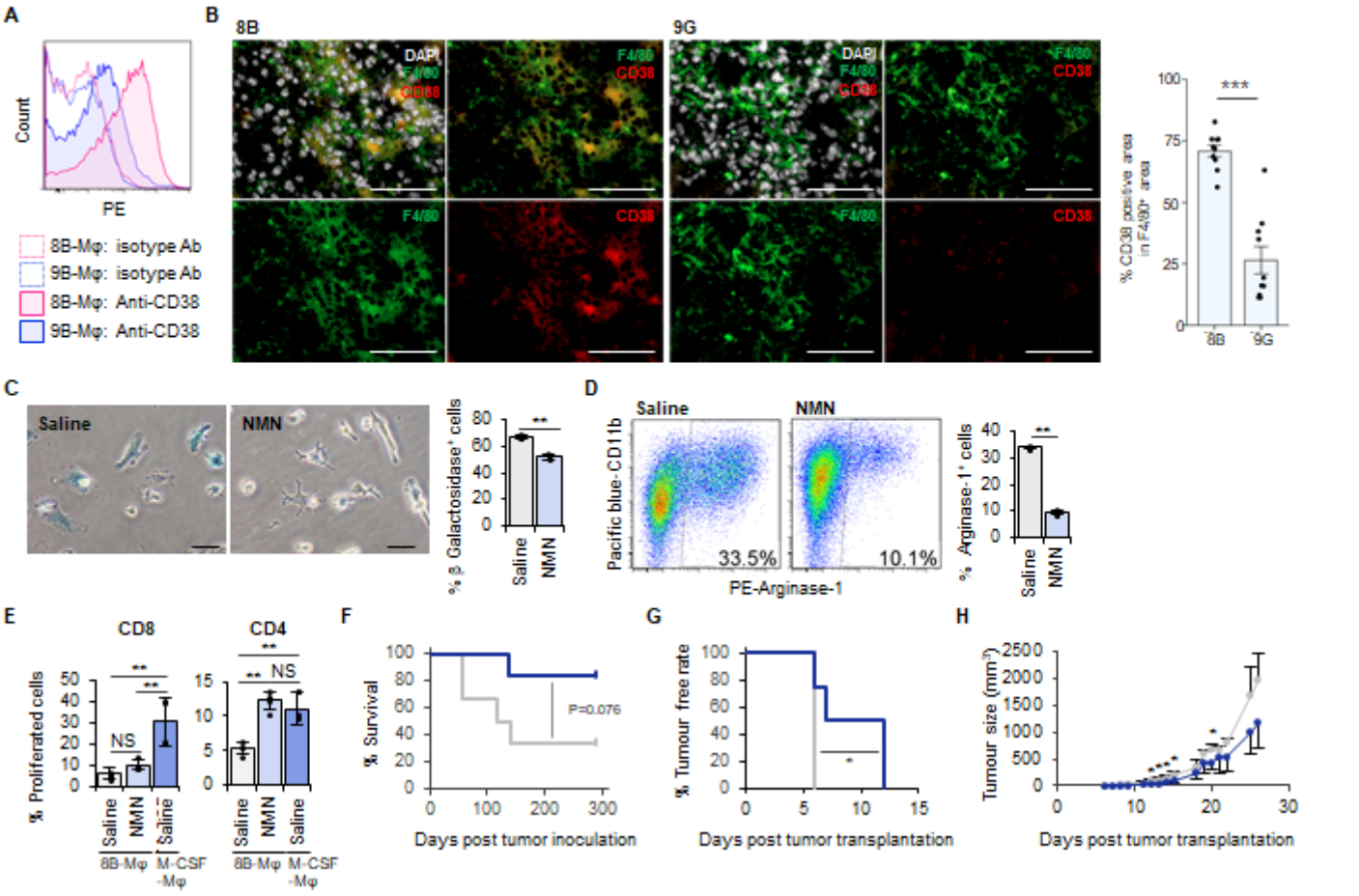

Figure 4

Supplementation of NMN inhibited Mφs to go into a senescence-like state, induced expression of an immunosuppressive phenotype and improved survival of immunocompetent mice after lethal inoculation of tumour cells

We screened expressed surface proteins on 8B-sup cultured senescence-like Mφs. **A**, 8B- or 9G-supernatant-cultured Mφs were stained with anti-CD38 mAb. **B,** Mouse brains that were given 8B or 9G tumour cells 7 days earlier were stained with F4/80, CD38, and DAPI. The bar graph shows the proportion of CD38 positive area in the F4/80 positive area. Ten independent regions were analysed, and the means were compared using unpaired Student's *t*-test. ***p < 0.001. Each dot represents the % of CD38 positive area in F4/80$^+$ area in each sample. Bars; 100 mm. **C**, Splenic F4/80$^+$ cells were cultured in 8B-supernatant with/without nicotinamide mononucleotide (NMN) for 14 days followed by a SA-b-Gal assay. SA-b-Gal positive and negative cells in ten different views were counted; the proportion of positive cells was calculated from the total number. The bars indicate the mean (± SD) of % SA-b-Gal positive cells from three independent cultures. Each dot represents the % b-Galactosidase$^+$ cells in each independent culture. **p < 0.01, Student's *t*-test. **D**, Arginase-1 expression of the generated cells in **B**. The bars indicate the mean (± SD) from three independent flow cytometry analysis. Each dot represents the % of Arginase-1$^+$ cells in each independent culture. **p < 0.01, Student's *t*-test. **E**, Assessment of NMN treatment on the

immune activating capacity of 8B-Mφs. The allogeneic T cell activating capacity of Mφs were evaluated by CFSE assay. 8B-Mφs were induced with/without NMN. M-CSF induced Mφ was used as positive control. The Mφs and CFSE-labelled $Thy1^+$ T cells from BALB/c were co-cultured for 4 days; then stained with CD4 and CD8, their proliferation was analysed by CFSE reduction. The bars indicate the mean (± SD) from four independent flow cytometry analysis. Each dot represents the % of proliferated cells in each culture. **p < 0.01, NS: not significant, Tukey-Kramer HSD test. **F**, 8B cells (1×10^4) were transplanted into the C57BL/6 mouse brain. NMN or saline was inoculated twice per week. Mouse survival was observed. The dark blue line shows NMN-treated mice (n = 6); the grey line shows saline-treated mice (n = 6). *p < 0.05, log-lank test. **G**, CT26 cells were subcutaneously injected into syngeneic immunocompetent BALB/c mice. NMN or saline was inoculated three times per week until death. Tumour initiation was evaluated using ocular inspection and palpation. The dark blue line indicates NMN-treated mice (n = 4); the grey line indicates saline-treated mice (n = 4). **p < 0.01, log-lank test. **H**, The average tumour size (± SD) of CT26 transplanted mice described in **G**. The dark blue line indicates NMN-treated mice (n = 4); the grey line indicates saline-treated mice (n = 4). *p < 0.05, Student's *t*-test.

Supplementary Files

This is a list of supplementary files associated with this preprint. Click to download.

- 221022SupFiglegends.docx
- 221022SupMatelialsandMethods.docx
- 221022ver23SupFigs.pptx